Enhancement of coercivity in the nanocomposite $R_{40}Fe_{30}Co_{15}Al_{10}B_5$ (R = Nd, Pr)

2003 J. Phys.: Condens. Matter 15 5615

(http://iopscience.iop.org/0953-8984/15/32/320)

INSTITUTE OF PHYSICS PUBLISHING JOURNAL OF PHYSICS: CONDENSED MATTER

J. Phys.: Condens. Matter **15** (2003) 5615–5620 PII: S0953-8984(03)63825-7

Enhancement of coercivity in the nanocomposite $R_{40}Fe_{30}Co_{15}Al_{10}B_5$ (R = Nd, Pr)

S Sab[1], L Bessais[1,3], C Djéga-Mariadassou[1], N H Dan[2] and N X Phuc[2]

[1] LCMTR, UPR209, CNRS, 2/8 rue Henri Dunant, BP 28 F-94320 Thiais, France
[2] Institute of Materials Science, NCST, Hoang Quoc Viet Road, Viet Nam

E-mail: bessais@glvt-cnrs.fr

Received 22 May 2003
Published 1 August 2003
Online at stacks.iop.org/JPhysCM/15/5615

Abstract

The structure and magnetic properties of high-energy-milled $R_{40}Fe_{30}Co_{15}Al_{10}B_5$ (R = Nd, Pr) have compounds been investigated by means of x-ray diffraction, high-resolution transmission electron microscopy, magnetic measurements, and Mössbauer spectroscopy. The x-ray diffractograms of the as-milled alloys are typical for the amorphous state. Nanocrystalline $R_2(Fe, Co, Al)_{14}B$ coexisting with $R_6(Fe, Co)_{13-x}Al_{1+x}$ is observed after recrystallization at 750 °C. The mechanically milled amorphous samples exhibit a relatively moderate coercivity of ≈6.5 kOe at room temperature and a Curie temperature (T_C) ≈ 650 K. After subsequent annealing, both systems show hard magnetic behaviours—such as a record-high coercivity of 29 kOe with approximately the same T_C as for amorphous as-milled alloys.

Rare-earth-based R–Fe–Al bulk amorphous alloys have attracted much attention, mainly due to their great glass-forming ability and their room temperature hard magnetic properties, coupled to high fracture strength and good corrosion resistance. Since the first investigation by Inoue *et al* [1], a lot of works have been devoted to Nd–Fe–Al alloys obtained by melt spinning [2–6] or suction casting [7, 8] with various compositions.

The best hard magnetic properties of $Nd_{60}Fe_{30}Al_{10}$ were explained by the existence of dispersed nanocrystalline phases embedded in an amorphous matrix [6, 8]. However, multimagnetic phase behaviour was clearly identified in low-quenching-rate ribbons [3] and, whatever the cooling rate, the samples contain two main phases: one soft phase and one hard magnetic phase, with intrinsic coercivity of 3.5 kOe at room temperature (RT).

In a further step, boron has been added to improve the amorphization ability. The substitution of B for Al leads to an enhancement of the hard magnetic properties via $Nd_2Fe_{14}B$ [7]. More recently, Kumar *et al* [9] obtained with mould-cast samples of

[3] Author to whom any correspondence should be addressed.

$Nd_{40}Fe_{40}Co_5Al_8B_8$ a coercivity of 3.37 kOe at RT; in contrast, their mechanically alloyed amorphous samples are soft magnetic with a maximum coercivity of 0.13 kOe.

Few studies have been performed up to now on amorphous Pr-based alloys. However, Pr is very attractive due to its electronic properties being close to those of Nd. A milling technique for the preparation of hard magnetic rare-earth–transition metal materials was successfully developed several years ago for high-coercivity magnets. It is a cost-effective alternative to rapid quenching and allows the production of large batches of homogeneous materials. So far, no investigation has been performed on mechanically milled amorphous R–Fe–Al alloys with subsequent annealing.

Our objective is to create an amorphous state by mechanical alloying and perform a controlled *in situ* nanocrystallization of the amorphous as-milled alloys in order to improve their magnetic properties to the standard required in many applications, especially in magnetic recording media and permanent magnets. In the present work we present results from x-ray diffraction (XRD) and high-resolution transmission electron microscopy (HRTEM), combined with energy-dispersive x-ray analysis (EDX) and measurements of the Curie temperature (T_C) and coercivity (H_C), coupled with Mössbauer spectroscopy, on transition metal-rich compositions of R–Fe–Co–Al–B (R = Nd, Pr).

The samples $R_{40}Fe_{30}Co_{15}Al_{10}B_5$ (R = Nd, Pr) were prepared by high-energy ball-milling of boron with pre-melted R–Fe–Co–Al as described previously [11, 12]. The as-milled powders were crystallized at temperatures in the range 300–750 °C for 20 min. The crystalline structures were checked by means of XRD using Cu Kα radiation. HRTEM micrographs and EDX analysis were performed with a JEOL 2010. The sample powders were imbedded in epoxy and microtomed to a thickness around 70 nm prior to imaging. The temperatures T_C were measured with a differential sample magnetometer under 1 kOe, while the M–H hysteresis curves were obtained, at RT, with a SQUID magnetometer in a field up to 55 kOe. ^{57}Fe Mössbauer spectra were collected, at RT, using a constant-acceleration spectrometer with a 50 mCi rhodium-matrix Co source.

The XRD data were fitted by Rietveld analysis (RA) using the FULLPROF computer code on the assumption of a Thompson–Cox–Hastings line profile. This permits the refinement of each coexisting phase, takes into account the broadening of the diffraction lines induced by grain size and strain effects, and evaluates the weighted relative contents (wt%) of the various phases [13]. A weighed quantity of silicon was used as standard to define the amount of the amorphous phase in the annealed state [14] and moreover permitted us to define the unit cell parameter within the accuracy ±0.003 Å.

The XRD patterns of the as-mechanically milled powders are typical of amorphous phase. No obvious diffraction peaks corresponding to crystalline phases were observed. The diffraction peaks become more pronounced with increasing annealing temperature. The annealing at 750 °C for 20 min induces the formation of two phases (figure 1), $P4_2/mnm$ $R_2(Fe, Co, Al)_{14}B$ and $I4/mcm$ $R_6(Fe, Co)_{13-x}Al_{1+x}$, with lattice parameters reported on table 1. A small amount (around 3 wt%) of R_2O_3 is also observed. For both Pr- and Nd-based alloys the derived cell parameter a is lower than that of $R_2Fe_{14}B$. It reflects mainly Co substitution, while the cell parameter c being higher than that of $R_2Fe_{14}B$ is mainly due to Al substitution [15, 16]. The RA gives the relative contributions of the two phases as equal to 40 and 60 wt% for respectively $R_6(Fe, Co)_{13}Al$ and $R_2(Fe, Co, Al)_{14}B$ with a grain size around 25–30 nm. The amount of the amorphous part compared to this crystalline contribution is around 35 wt%.

HRTEM images were taken to study the morphology and the structure of both alloys. Interatomic distances d_{hkl} are calculated using a simulated electron diffraction pattern by means of a Fourier transform, derived from the lattice fringe of the HRTEM images. The micrographs

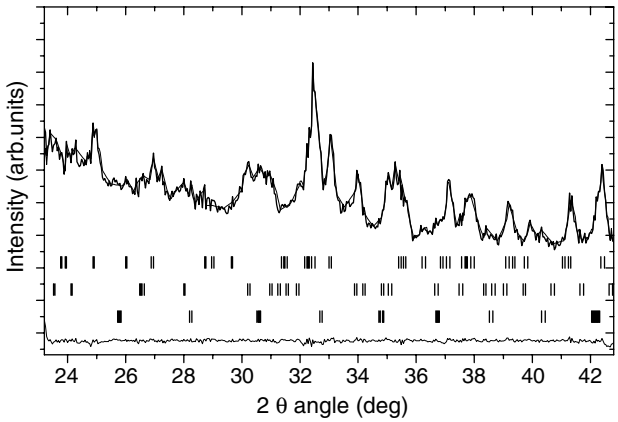

Figure 1. RA for Pr–Fe–Co–Al–B, as an example. The sets of ticks refer, from top to bottom, to $Pr_2(Fe, Co, Al)_{14}B$, $Pr_6(Fe, Co)_{13-x}Al_{1+x}$, and Pr_2O_3.

Table 1. Unit cell parameters of $R_{40}Fe_{30}Co_{15}Al_{10}B_5$ annealed at 750 °C. The accuracy is ±0.003 Å.

R	Phase	*a* (Å)	*c* (Å)
Nd	$Nd_6(Fe, Co)_{13-x}Al_{1+x}$	8.316	22.578
	$Nd_2(Fe, Co, Al)_{14}B$	8.776	12.268
Pr	$Pr_6(Fe, Co)_{13-x}Al_{1+x}$	8.338	22.582
	$Pr_2(Fe, Co, Al)_{14}B$	8.786	12.307

clearly indicate three kinds of region (figure 2). There are two distinct crystalline areas. (i) Region (1) is representative of $R_2Fe_{14}B$ with grain sizes in the range of 25–30 nm. (ii) Region (2) shows small particles of $R_6(Fe, Co, Al)_{14}$ with an average diameter around 7 nm. However, some larger particles of $R_6(Fe, Co, Al)_{14}$, around 30 nm, have also been observed by HRTEM according to XRD diagrams. A third region (region (3)) corresponds to a glassy area characterized by a broad electron diffraction ring, revealed by EDX analysis to be Co and R rich, and iron free. These results confirm the structure characteristics of both crystalline phases given by RA.

The T_C-values of the Nd–Fe–Co–Al–B and Pr–Fe–Co–Al–B alloys before and after annealing are respectively 645, 630 K and 650, 625 K. These values are higher than T_C for crystalline $Nd_2Fe_{14}B$ ($T_C = 585$ K). The temperature dependence of the magnetization (from 293 to 900 K), for amorphous and annealed samples, indicates only one ferromagnetic phase $R_2(Fe, Co, Al)_{14}B$. The tetragonal phase $R_6(Fe, Co)_{13-x}Al_{1+x}$ is known to order antiferromagnetically [17]. This agrees with the absence of other order transitions in the M–T curves. ^{57}Fe Mössbauer spectroscopy corroborates these results.

The Mössbauer spectra of both Pr- and Nd-based alloys are comparable. Two contributions explain the spectrum of as-milled amorphous forms: on the one hand, a magnetic contribution of 70% relative to a distribution of the hyperfine field with mean hyperfine field $\langle H_{HF}\rangle = 223$ kOe correlated with a distribution of isomer shift with $\langle\delta\rangle = -0.071$ mm s^{-1}; on the other hand, a paramagnetic contribution with an abundance of 30% and $\langle\delta\rangle = -0.034$ mm s^{-1}. In the spectra of the annealed samples, the $R_2(Fe, Co, Al)_{14}B$ phase contributes to the magnetic part with abundances of 49 and 51% respectively for R = Nd and Pr. The remaining part can be assigned to the $R_6(Fe, Co)_{13-x}Al_{1+x}$ phase, which results from two contributions, a magnetic

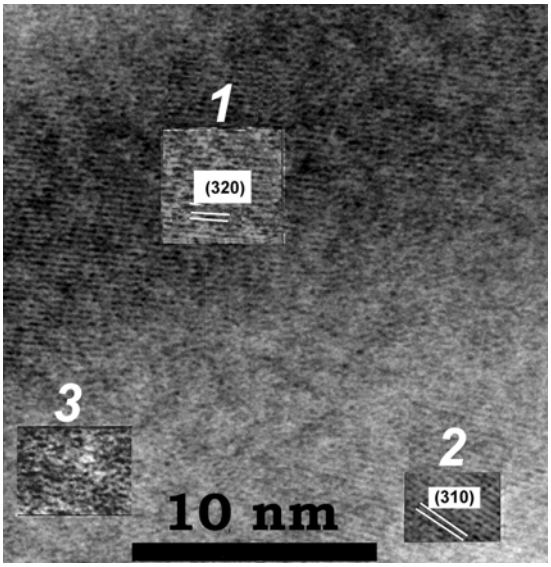

Figure 2. A HRTEM image of Pr–Fe–Co–Al–B showing crystalline ((1) and (2)) and amorphous (3) regions (see the insets).

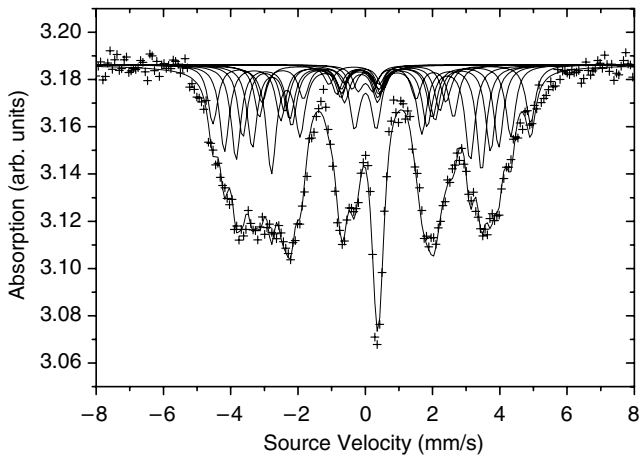

Figure 3. The RT Mössbauer spectrum of Nd–Fe–Co–Al–B annealed 20 min at 750 °C, as an example.

one with an abundance of 42 or 9% of either a paramagnetic or a superparamagnetic component (see figure 3 for an example). HRTEM confirms the existence of small monodomain particles.

For all samples, significant increase in the RT coercivity was found after heat treatments up to 750 °C. In contrast, all samples annealed above this temperature present a lower H_C. The coercivity decreases with increasing annealing temperature due to an increase in crystalline grain size [18, 19]. M–H hysteresis curves, measured at RT, for mechanically milled $Nd_{40}Fe_{30}Co_{15}Al_{10}B_5$ and $Pr_{40}Fe_{30}Co_{15}Al_{10}B_5$ (amorphous) are shown in figures 3(a) and (b). The Nd-based alloy exhibits a coercivity H_C of 6.4 kOe with a remanent induction B_R of 2.7 kG. These values are the highest measured in Nd-based bulk amorphous alloys at

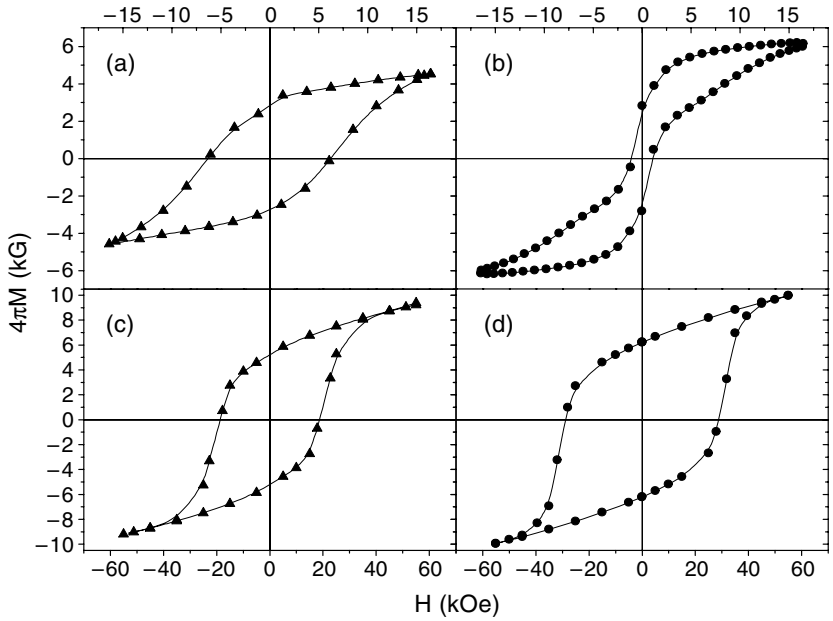

Figure 4. Hysteresis loops at RT of $Nd_{40}Fe_{30}Co_{15}Al_{10}B_5$, (a) as-milled amorphous, (c) annealed at 750 °C; and of $Pr_{40}Fe_{30}Co_{15}Al_{10}B_5$, (b) as-milled amorphous, (d) annealed at 750 °C.

RT—however, obtained up to now with other technique [9]. Nevertheless, aluminium was found [10] to enhance the coercivity in sintered Nd–Fe–B magnets up to 20 kOe.

The Pr-based amorphous alloys, never prepared before, show smaller H_C and higher magnetization. In figures 3(c) and (d) we report the hysteresis loops of the samples investigated, heat treated at 750 °C. No shoulder in the demagnetization curve nor small steps near $H = 0$ are observed. This means that the samples contain only one phase responsible for the intrinsic magnetic properties.

In the case of Nd–Fe–Co–Al–B, H_C increases to 19 kOe and $4\pi M_R = 5.3$ kG. Pr–Fe–Co–Al–B alloys show a higher remanent induction of 6.4 kG with a drastic increase of coercivity to 29 kOe. The coercivity shows a maximum, due to the optimal microstructure, for a grain size in the range of 25–30 nm checked by HRTEM. The high coercivity values at RT for the annealed alloys can be explained by a domain wall pinning model. The $R_6(Fe, Co)_{13-x}Al_{1+x}$ and $R_2(Fe, Co, Al)_{14}B$ phases, being magnetically different, act as domain wall pinning centres. The increase in crystallinity with increasing annealing temperature enhances the domain wall pinning and, hence, the coercivity.

To summarize, these R–Fe–Co–Al–B alloys prepared by a simple route of nanocrystallization, in large homogeneous amounts, are particularly promising in the Pr case. This rare earth, more rarely used, leads to improved hard magnetic behaviour with T_C equal to 625 K and a high coercivity of 29 kOe. Such systems, elaborated by this method, open a route to promising magnetic applications.

References

[1] Inoue A, Zhang T and Takeuchi A 1997 *IEEE Trans. Magn.* **33** 3814
[2] Ding J, Si L, Li Y and Wang X Z 1999 *Appl. Phys. Lett.* **75** 1

[3] Dan N H, Phuc N X, Hong N M, Ding J and Givord D 2001 *J. Magn. Magn. Mater.* **226** 1385
[4] Lupu N, Chiriac H, Takeuchi A and Inoue A 2001 *Mater. Res. Soc. Symp. Proc.* **674** 271
[5] Sun Z G, Löser W, Eckert J, Muller K H and Schultz L 2002 *J. Appl. Phys.* **91** 9267
[6] Kramer J, O'Connor A S, Dennis K W, McCallum R W, Lewis L H, Tung L D and Duong N P 2001 *IEEE Trans. Magn.* **37** 2497
[7] Chau N, Luong N H, Huu C X, Phuc N X and Dan N H 2002 *J. Magn. Magn. Mater.* **242** 1314
[8] Schneider S, Bracchi A, Samwer K, Seibt M and Thiyagarajan P 2002 *Appl. Phys. Lett.* **80** 1749
[9] Kumar G, Eckert J, Roth S, Löser W, Ram S and Schultz L 2002 *J. Appl. Phys.* **91** 3764
[10] Zhang M, Ma D, Jiang X and Liu S 1985 *Proc. 8th Int. Workshop on Rare-Earth Magnets (University of Dayton, Dayton, OH)* pp 541–52
[11] Djéga-Mariadassou C, Bessais L, Nandra A, Grenèche J M and Burzo E 2001 *Phys. Rev.* B **65** 014419
[12] Bessais L, Sab S, Djéga-Mariadassou C and Grenèche J M 2002 *Phys. Rev.* B **66** 054430
[13] Rodríguez-Carvajal J, Fernandez-Diaz M T and Martinez J L 1991 *J. Phys.: Condens. Matter* **3** 3215
[14] Zevin L S and Kimmel G 1995 *Quantitative X-ray Diffractometry* (New York: Springer)
[15] Herbst J F and Yelon W B 1986 *J. Appl. Phys.* **60** 4224
[16] Croat J J, Herbst J F, Lee R W and Pinkerton F E 1984 *Appl. Phys. Lett.* **44** 148
[17] de Groot C H, Buschow K H J and de Boer F R 1998 *Phys. Rev.* B **57** 11472
[18] Bessais L and Djéga-Mariadassou C 2001 *Phys. Rev.* B **63** 54412
[19] Zhang J X, Bessais L, Djéga-Mariadassou C, Leroy E, Percheron-Guégan A and Champion Y 2002 *Appl. Phys. Lett.* **80** 1960